

Monte Carlo simulations of liquid spreading on a solid surface: Effect of end-group functionality

X. Ma,^{1,*} C. L. Bauer,¹ M. S. Jhon,² J. Gui,³ and B. Marchon⁴

¹Department of Materials Science and Engineering, Carnegie Mellon University, Pittsburgh, Pennsylvania 15213

²Department of Chemical Engineering, Carnegie Mellon University, Pittsburgh, Pennsylvania 15213

³Seagate Recording Media, 47010 Kato Road, Fremont, California 94538

⁴IBM, Almaden Research Center, 650 Harry Road, San Jose, California 95120

(Received 22 January 1999; revised manuscript received 26 May 1999)

The spreading of liquid droplets composed of molecules with or without reactive end groups over a solid surface has been studied using Monte Carlo simulations. For molecules without reactive end groups, a molecular layering in the spreading profiles is predicted, depending on the ratio of the magnitude of intermolecular interactions to thermal energy. As intermolecular interactions become smaller than thermal energy, the layered structure vanishes. For molecules with reactive end groups, interactions between end groups and between end groups and the surface complicate the situation. By assuming an end-to-end interaction between molecules and the pinning of end groups to the surface, a complex layered structure is obtained. Our simulation predicts spreading profiles that accurately describe the broad spectrum of data obtained from scanning microellipsometry for perfluoropolyalkylethers with and without reactive end groups. [S1063-651X(99)09911-0]

PACS number(s): 68.10.Gw, 05.50.+q, 68.10.Jy, 68.15.+e

I. INTRODUCTION

Recently, the spontaneous spreading of ultrathin liquid films on solid surfaces at the microscopic level has gained considerable attention. A fundamental understanding of the interactions between liquid molecules and solid surfaces governing spreading is important in many technological applications, such as paints, adhesion, lubrication, etc. [1–3]. The spreading of small drops of polydimethylsiloxane (PDMS) on solid surfaces has been studied intensively [4–9]. It was reported that a molecular layering with a layer thickness of approximately 0.7 nm developed for PDMS terminated with trimethyl groups on silica. However, PDMS terminated with hydroxyl groups did not exhibit molecular layering; instead, an anchored layer with a thickness close to the radius of gyration was observed. Similar results were reported for the spreading behavior of PFPE's with reactive end groups, such as Zdol (terminated with hydroxyl groups), AM2001 (terminated with piperonyl groups), and Ztetraol (terminated with propylene glycol ether groups) [10–12]. Our study demonstrates that films spread with a smooth film front for nonfunctional PFPE Z, and no molecular layering is observed. However, for functional Zdol, a complex layering structure with unequal thicknesses on the order of the radius of gyration is observed, with the first layer being “diffusive,” and subsequent layers exhibiting sharp steps of about twice the thickness of the first layer, as shown in Fig. 1 [13].

Since the molecular layering in the spreading of PDMS liquid on silica surfaces was reported [4–9], many computer simulations have been conducted to examine molecular layering using Monte Carlo (MC) and molecular dynamics (MD) methods [14–24]. In MD simulations, by introducing a Lennard-Jones potential, agreement with experimental observations was obtained. For a simple liquid [14,15], the move-

ment of the liquid front demonstrates a $(\log_{10}t)^{1/2}$ time dependence, in contrast to experimental observations, where the square root of time $t^{1/2}$ dependence is observed. Bekink *et al.* [22] also studied the spreading of simple liquids on solid surface. They reported that the $(\log_{10}t)^{1/2}$ dependence is due to the porosity of the lattice assumed in the previous work.

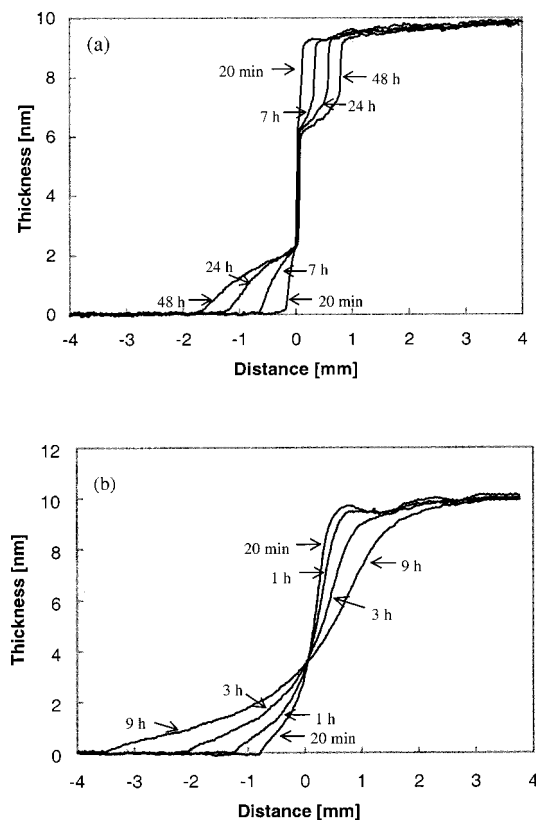


FIG. 1. Spreading profiles of (a) Zdol with an initial thickness of 9.8 nm, at times of 20 min, 7 h, 24 h, and 48 h; and (b) Z with an initial thickness of 10 nm, at times of 20 min, 1 h, 3 h, and 9 h.

*Present address: Seagate Recording Media, 47010 Kato Road, Fremont, CA 94538.

When the nearest-neighbor distance is reduced, $t^{1/2}$ dependence is obtained. The $(\log_{10}t)^{1/2}$ dependence is also attributed to the insufficient molecules in the drop reservoir being considered in the simulations, which will result in a mixture of two $t^{1/2}$ regimes [20]. The spreading of polymeric liquids was studied by several authors [17,20,21,24]. Nieminen and Ala-Nissila [17] reported that there is an initial linear growth in time ($x \sim t$), crossing over at some characteristic time to the $t^{1/2}$ diffusion law, which agrees with the experimental observations reported by O'Connor *et al.* [10].

The mechanism of fluid spreading has also been studied using MC simulations, with the adoption of the Ising model [18,19,23], and molecular layering was obtained. Crossover from a linear time growth of precursor spreading to a $t^{1/2}$ growth was report in Ref. [23]. It is believed that, at early times, spreading is dominated by fluid particles flowing down along the droplet boundary, demonstrating a constant-speed spreading of the precursor layer. At later times, spreading is dominated by particles migrating from the edge of the second layer and randomly walking on the first layer until holes are encountered or the rough edge of the precursor layer is reached. It was found that this transient crossover time is dependent on the initial contact angle. A longer transient time is expected for larger contact angles.

Previous investigators focused mainly on molecules without reactive end groups. Molecular layering in spreading appears to be universal regardless of molecular structure, lattice geometry, and system size. Our experimental observations, however, show no layering in the spreading of nonfunctional Z, while it is clearly observed for PFPE's with reactive end groups [13]. In this work, the spreading of liquid over a solid surface is qualitatively studied using the MC method to interpret the observations of spreading of PFPE's with and without reactive end groups.

II. THE MODEL

Similar to the model used by previous investigators [18,19,23], a solid-on-solid approximation was employed to represent a liquid droplet on a solid surface. In this work a three-dimensional cubic lattice above a structureless substrate was assumed. Molecules are represented by structureless particles and occupy lattice sites to form a droplet. Monte Carlo simulations with Kawasaki dynamics were then performed with particle conservation. After the droplet has been deposited, it will spread according to the principle of energy minimization. The Hamiltonian of the system to be investigated can be written as

$$H = H_{m,m} + H_{m,s} + H_{e,e} + H_{e,s}, \quad (1)$$

where $H_{m,m}$, $H_{m,s}$, $H_{e,e}$, and $H_{e,s}$ denote the interactions between molecules, between molecules and the substrate, between end groups, and between end groups and the substrate, respectively. A lattice gas model, which draws an analogy to the Ising model, assigns a filled lattice site with a spin $S = 1$, and an empty site with a spin $S = 0$. Molecules interact with nearest neighbors by the coupling constant J . Here, $J > 0$ means that attractive intermolecular interactions occur, resulting in film cohesion. The interaction between molecules can be expressed by

$$H_{m,m} = -\frac{J}{2} \sum_{i,j,k} S_{i,j,k} S_{i\pm 1,j\pm 1,k\pm 1}, \quad (2)$$

where i , j , and k are the indices along three orthogonal directions of the three-dimensional lattice. Attractive van der Waals interactions assigned between molecules and the substrate are given by

$$H_{m,s} = \sum_{i,j,k} V(k) S_{i,j,k} \quad (3)$$

with

$$V(k) = -\frac{A}{k^3}, \quad (4)$$

where the interaction parameter A is of the order of the Hamaker constant A_H [23].

An explicit expression for the interactions between end groups, and between end groups and the substrate, is not easily obtained. Experimental results show that molecules with reactive end groups behave differently in spreading from those without reactive end groups [13]. A complex layering develops during the spreading of molecules with reactive end groups; layer thickness is on order of the radius of gyration, and the thicknesses of layers are not equal, as the second layer has nearly twice the thickness of the first layer (Fig. 1). This agrees with the result reported by Tyndall, Karis, and Jhon [25], where the dependence of the polar component of the surface energy on the thickness of Zdol film on an amorphous carbon surface exhibits several minima. The distance from the first minimum to the second is approximately twice the thickness of the first minimum, indicating that end groups prefer to stay together in order to reduce the system energy. A possible molecular conformation of the films has been proposed [26], where Zdol molecules in the first monolayer have a coil conformation with the end group anchored to the carbon surface and the backbone pointing away from the surface. The second layer is composed of two molecular layers with a high concentration of end groups in the middle.

Based on this analysis, a model was proposed by representing the orientation of the end group by the direction of an assigned spin. The projection of S in the direction of z (S^z), which is perpendicular to the substrate, represents the orientation of the end group. $S^z = 1$ denotes an upward-pointing end group, and $S^z = -1$ represents a downward-pointing end group. End-to-end interactions between spins along the direction normal to the surface are assumed, since interactions between end groups only occur when they meet. Thus, the interaction between reactive end groups can be expressed as

$$H_{e,e} = -\frac{K}{4} \sum_{i,j,k} (S_{i,j,k}^z + 1)(S_{i,j,k+1}^z - 1) S_{i,j,k} S_{i,j,k+1}, \quad (5)$$

where K is the coupling constant between end groups. Here, $K > 0$, indicating that it is favorable for end groups to stick to each other. The substrate serves to pin the spins to the surface, so that the spins of molecules on the surface will point

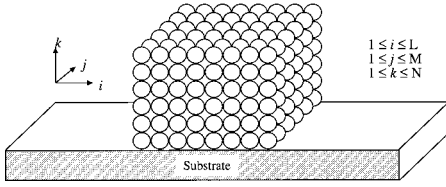


FIG. 2. Schematic of the simulated lattice.

down with $S^z = -1$. This represents the anchoring of end groups to the surface. The term $H_{e,s}$ is given by

$$H_{e,s} = \sum_{i,j,k} W(k) S_{i,j,k}^z, \quad (6)$$

where $W(k)$ is the interaction energy between the end groups of one molecule and the substrate and is expressed as

$$W(k) = -W \delta_{k,1}, \quad (7)$$

where $\delta_{k,l}$ is the Kronecker delta, and $W > 0$ in this work. From Eqs. (1)–(7), we obtain

$$\begin{aligned} \frac{H}{kT} = \frac{J}{kT} & \left[-\frac{1}{2} \sum_{i,j,k} S_{i,j,k} S_{i\pm 1, j\pm 1, k\pm 1} - \frac{A}{J} \sum_{i,j,k} \frac{S_{i,j,k}}{k^3} \right. \\ & - \frac{K}{4J} \sum_{i,j,k} (S_{i,j,k}^z + 1)(S_{i,j,k+1}^z - 1) S_{i,j,k} S_{i,j,k+1} \\ & \left. - \frac{W}{J} \sum_{i,j,k} S_{i,j,k}^z \delta_{k,1} \right]. \quad (8) \end{aligned}$$

It should be pointed out that the interaction parameters, J , A , K , and W are introduced here to approximate the cohesive (molecule/molecule) and adhesive (molecule/surface) interactions. Since the detailed structure of the molecule is not considered in this model, those parameters should therefore be viewed as resulting from an integration over its internal degrees of freedom.

During the MC simulation, the probability P of the interrogated molecule moving to the nearest empty site is given by

$$P = \frac{1}{1 + \exp(\delta H/kT)}, \quad (9)$$

where $\delta H = H^f - H^i$, and H^i and H^f are the Hamiltonians of the system before and after a movement is made, respectively. The time step for each cycle is arbitrary.

A three-dimensional lattice with dimensions of $L \times M \times N$ is generated, where M is chosen to be in the direction of the periodic boundary condition. An initial droplet is then formed on the substrate, as shown schematically in Fig. 2. During each cycle, every lattice site is randomly interrogated. If the site is empty, the interrogation goes to the next randomly selected site. If the site is occupied, a direction is randomly selected. If the projected nearest site is filled, the interrogation goes to next randomly selected site. If not, the probability P is calculated using Eq. (9), and a random number R between 0 and 1 is generated. If $R > P$, no movement is made. If $R \leq P$, one movement is made.

Two types of liquid molecules were investigated: molecules with nonreactive end groups and molecules with reactive end groups. When the simulation is complete, the particles without nearest neighbors as well as particle clusters, which have no connection with the droplet, are regarded as evaporated “gas molecules” and removed from the lattice. Spreading profiles are obtained by summing the number of particles in the plane of $M \times N$ along the direction of L , thereby simulating thickness profile measurements by ellipsometry.

The size of the lattice was chosen as $101 \times 10 \times 20$ with 1050 molecules, or $201 \times 10 \times 20$ with 5050 molecules. To achieve good statistics, the final spreading profiles are obtained by averaging over ten runs.

III. RESULTS

A. Spreading of nonfunctional liquid

For nonfunctional liquids, the interactions associated with end groups in Eq. (8) are set to zero ($K = W = 0$). Since upward movement of molecules is permitted in this simulation, the choice of J has a significant effect on spreading behavior. In particular, the value of J/kT should be large enough to maintain a low vapor pressure, and if J/kT is too small ($\ll 1$), evaporation will be severe, as discussed in Ref. [23]. Figure 3 shows the spreading profiles at time $t = 10\,000$, $50\,000$, and $100\,000$ MC steps with $J/kT = 2$ for (a) $A/J = 100$, (b) $A/J = 7.5$, and (c) $A/J = 2.5$. Error bars (1σ) are displayed in Fig. 3(a), and have been found to be of the same order of magnitude for the rest of the simulation profiles. For clarity, only averages will therefore be displayed throughout the rest of the paper. In this range of interaction parameters, it was found that the percentage of evaporated molecules was always less than 0.5%. Figure 3 shows that molecular layering develops with time. At small times, only the first layer is visible; however, as time progresses, second and third layers become visible.

During the spreading process, several mechanisms may occur: (1) molecules on the edge will first break several bonds with other molecules in the film and move outwards. Due to the van der Waals force exerted by the substrate, those molecules will tend to move downward towards the attractive substrate to form a precursor layer. (2) After the precursor layer has been formed, molecules from the film will move down toward and then diffuse on top of the precursor layer until they find a vacancy to fill or fall over the edge of the precursor layer. (3) Molecules can also evaporate, and remain in the atmosphere. Some molecules could fall over the layers and substrate. This process is energetically unfavorable for sufficiently large J and A . The overall picture is that spreading proceeds with the migration of molecules from the top to the lower layer, eventually reaching the substrate. From Fig. 3(c), it can be seen that, for a low value of A , only the first layer is visible. This is due to the small driving force for migration of molecules above the first layer. Upon increasing A , spreading of molecules in the upper layers increases and more layers are formed. Our simulation results agree qualitatively with earlier experimental results [4–7], as well as other computer simulation studies [16–24].

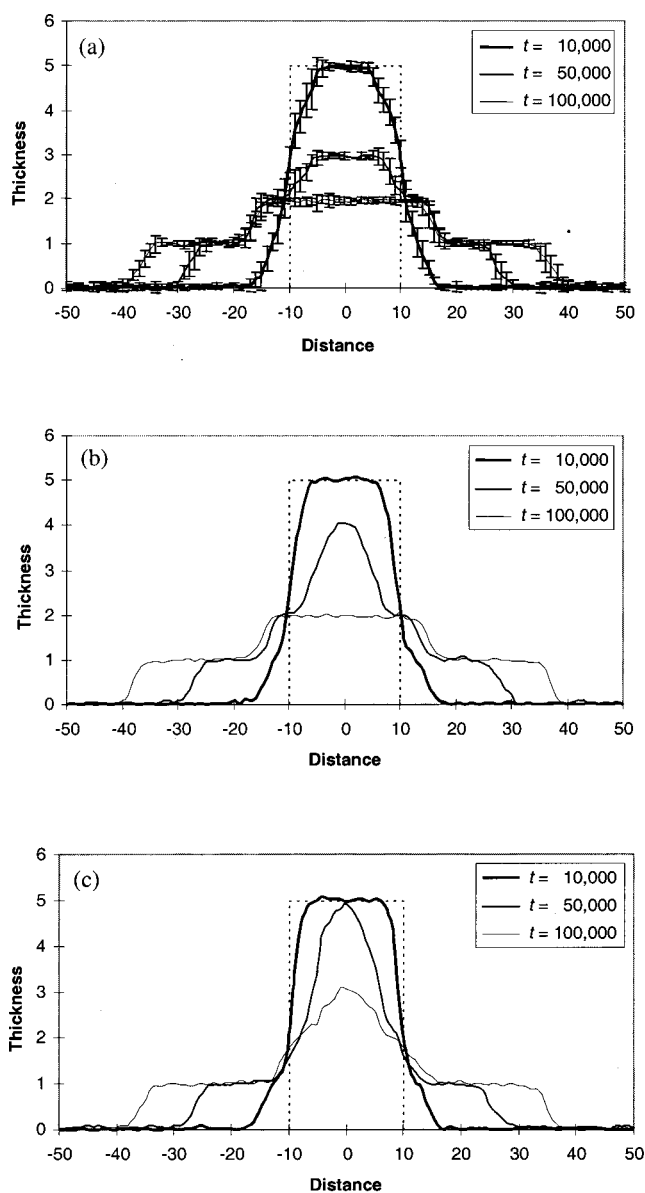


FIG. 3. Thickness profiles at time $t = 10\,000$, $50\,000$, and $100\,000$ MC steps. The dotted line represents the initial film profile. Both x and y axes are in molecular dimension units. The interaction parameters are $J/kT = 2$ with (a) $A/J = 100$, (b) $A/J = 7.5$, and (c) $A/J = 2.5$.

The effect of the strength of intermolecular interactions on spreading profiles was also investigated. Figure 4 shows spreading profiles for (a) $J/kT = 2$, (b) $J/kT = 1$, and (c) $J/kT = 0.5$ with $A/kT = 100$. For $J/kT = 2$, a layering similar to that in Fig. 3 develops from the initial film. As the interaction becomes weaker, the steps smooth out and evaporation becomes severe. The percentage of evaporated molecules increases from 0.3% at $J/kT = 2$ to over 10% at $J/kT = 0.5$. Layering in the spreading profiles was explained by an incompressible, stratified liquid model [27]. The spreading results from the affinity of molecules for the surface, and the first layer grows by molecules migrating down from the upper layers. A compact monolayer on the substrate will maintain the compactness of the upper layers. Therefore, layering can be observed if the liquid is nonvolatile in two

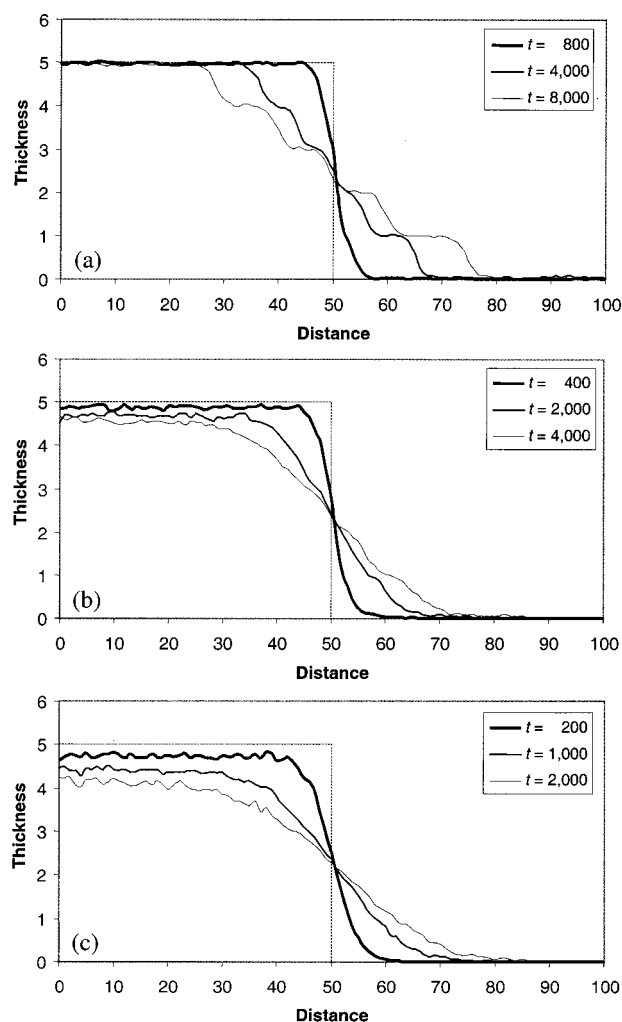


FIG. 4. Thickness profiles of films with five layers. The dotted line represents the initial film profile. Both x and y axes are in molecular dimension units. The interaction parameters are (a) $J/kT = 2$, (b) $J/kT = 1$, and (c) $J/kT = 0.5$ with $A/kT = 100$.

dimensions. When intermolecular interactions are comparable to the thermal energy, bonds in the film are easily broken. Molecules migrate faster on the surface as well as on top of the precursor layer, and the layers become less compact. Furthermore, molecules can also evaporate easily. Thus, the edge of the layer becomes less steep and layering becomes less pronounced. Bardon *et al.* [28] reported that layering in the profiles of Tetrakis(2-ethylhexoxy)silane and squalane at low temperature ($\sim 3^\circ\text{C}$) was smoothed out as temperature increased. In other words, at the same temperature, layering will be more pronounced for stronger intermolecular interactions.

B. Spreading of functional liquid

Until now the experimental or theoretical study of the spreading of functional liquids was rarely reported. This investigation explores the spreading behavior of a liquid droplet consisting of molecules with reactive end groups. Thus, the interaction parameters related to end groups, K and H , are nonzero. When a droplet with functional molecules is generated, the spin directions are randomly distributed, as shown schematically in Fig. 5(a). The spin system will then be re-

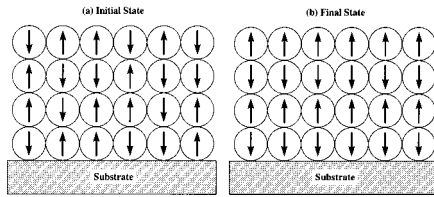


FIG. 5. Schematic diagram of the spin orientation of molecules on the surface at (a) the initial state and (b) the final state.

axed to minimize the energy. Upon reaching equilibrium, the final state [shown in Fig. 5(b)] should be achieved; here all of the spins in the first layer are pinned to the surface, and the spins of molecules in the upper layers are antiparallel to those of molecules in adjacent layers.

Figure 6 shows the simulation results of the spreading of liquid films with reactive end groups, where three sets of interaction parameters are selected: $J/kT=1$, $A/J=100$, and $W/J=10$ with (a) $K/J=2$, (b) $K/J=5$, and (c) $K/J=8$. The evaporation rate varies from 0.3% to 3% for the selected sets of parameters. From Fig. 6(b), a layering distinct from that observed in the profiles of nonfunctional liquid can be

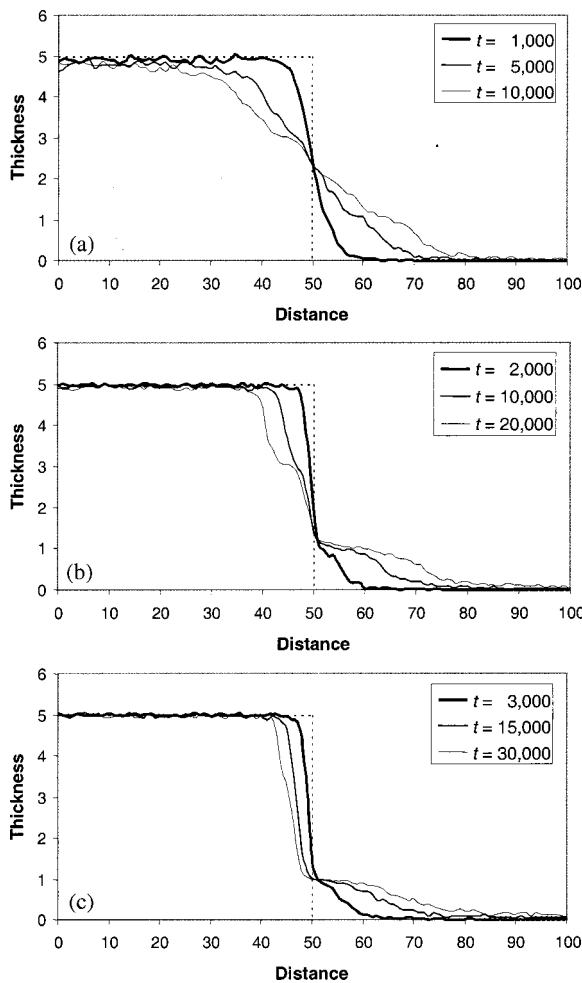


FIG. 6. Thickness profiles of liquid with reactive end groups. The dotted line represents the initial film profile. Both x and y axes are in molecular dimension units. The interaction parameters are $J/kT=1$, $A/J=100$, and $W/J=10$ with (a) $K/J=2$, (b) $K/J=5$, and (c) $K/J=8$.

readily identified: the first layer is diffusive and successive layers have relatively sharp edges. Layers have different thicknesses with subsequent layers being approximately twice as thick as the first layer. The picture of the spreading process in this case is that, as shown in Fig. 5(b), due to strong interactions between the end groups, it is difficult for molecules to escape from the binding of other molecules. Once a molecule is able to break free, it will quickly migrate to the substrate. While molecules at the surface of the droplet escape easier than those inside, the profiles will resemble the migration occurring pair by pair on top of the precursor layer. When the strength of interactions between end groups decreases, molecules can more easily break the bonds between end groups. Therefore, layering becomes smoothed out, as shown in Fig. 6(a). However, for stronger interactions, the probability of molecules to escape from the droplet decreases. The only opportunity for molecules to migrate is when there is a vacancy underneath them created after the molecules on the substrate migrate away from the edge of film. Thus, a profile with a steep edge on top of the diffusive precursor layer results, as shown in Fig. 6(c). It can be concluded that the strength of the interactions between end groups significantly affects layering in the spreading profiles of liquids with reactive end groups.

IV. DISCUSSION AND SUMMARY

Molecular layering in the spreading of liquids on solid surfaces is the most striking finding in recent studies. Numerous experimental and theoretical efforts have been made to understand the mechanism of layering. Our experiments show that layering is demonstrated by functional Zdol, but not by nonfunctional Z, as shown in Fig. 1. Our MC simulations demonstrate that, for nonfunctional liquids, interactions between the molecules, which determine the cohesion of liquids, plays a key role in layering. When the strength of the interactions is greater than the thermal energy of the system, the liquid in two dimensions is compact and molecular layering will develop in the spreading profiles. However, when the strength of the interactions is comparable to the thermal energy, the two-dimensional liquid becomes a two-dimensional gas. The diffusivity as well as volatility of the molecules will smooth out the edges of the layers. This is similar to the case of the spreading of nonfunctional Z investigated in our experiments. Looking strictly at the cohesive vs thermal interaction ratio J/kT , this result would imply that in the case of the PFPE backbone, the ratio should be lower than approximately 2 (Fig. 4), in order to match experimental profiles (Fig. 1). This is probably not the case, owing to the fairly strong cohesive energy of approximately 13.8 kJ/mol computed by Waltman, Tyndall, and Pacansky, [29], which would yield $J/kT \approx 5.7$. This somewhat contradictory finding might highlight the fact that this model assumes a rigid molecule, which is obviously not the case for a PFPE backbone where ether linkages provide great flexibility. It is also worth pointing out that these profiles were obtained with $A/kT=100$, which is probably on the upper range of values for this type of system. In fact, to within a geometrical factor, $A \approx A_H$ (Hamaker constant) $\approx 10^{19}$ J ≈ 60 kJ/mole, [30] which should bring this ratio closer to 25.

For molecules with reactive end groups, additional inter-

actions among end groups and between end groups and the substrate are present. After considering end-to-end spin interactions for the interaction between reactive end groups and a surface anchoring of the end groups, a complex layered structure similar to that observed in the spreading profiles of functional Zdol can be obtained by choosing appropriate interaction parameters. The range of interaction parameters that fits experimental profiles in a satisfactory fashion is for $W/J \approx 10$ and $K/J \approx 5$, which is fairly close to computed values of 6.6 and 3.6 reported by Waltman, Tyndall, and Pacansky [29]. This result brings some validity to this model, and confirms that the hydroxyl end groups in Zdol provide interactions that are overwhelmingly superior to backbone interactions. This is also consistent with the tribological performance reported by Mate [31]. To our knowledge, this is the first time that the spreading of liquid with reactive end groups has been investigated using computer simulations. Although the model is very simple since we did not incorporate detailed molecular structures and higher degrees of freedom for the end groups, our simulations qualitatively and semiquantitatively capture the essence of the experimental observation of spreading in PFPE's. The homogeneous surface approximation seems valid, since it reveals layering in the spreading profiles of functional polymeric liquids. However, in order to describe a realistic amorphous carbon surface, a population of pinning sites, as well as a distribution of pinning strengths, should be considered [32]. Incorporating surface heterogeneity would be helpful in explaining more complex experimental findings, such as the effect of hydrogenation and nitrogenation in carbon on the spreading of PFPE's [33].

In summary, the spreading of the liquids with multiple molecular layers was studied using the MC method by employing an Ising-like model. Results show that, for molecules without reactive end groups, a layered structure in the spreading profiles can be obtained for strong intermolecular

interactions. When the strength of the interactions decreases, the layered structure becomes less distinguishable, resulting in smooth thickness profiles. For functional liquids, the reactive end groups were represented by spins assigned to each molecule. By introducing an end-to-end interaction between molecules and the pinning of end groups to the surface, a layered structure similar to that observed in Zdol spreading profiles was obtained. A semiquantitative agreement with experimental data was obtained, using interaction energies published elsewhere. In the case of nonfunctionalized PFPE molecules, the model would predict layering at room temperature, when none is observed, using backbone-backbone cohesive energy available from the literature. This discrepancy probably arose from the great flexibility of the PFPE chain and its high number of ether linkages. However, the agreement with experimental data was satisfactory for functional PFPE, whose main interactions arise from the hydroxyl end groups. The purpose of this paper is not to provide a fully quantitative understanding of the spreading characteristics of functional liquids. The interaction parameters selected in this work, although in the proper range of values, would only be qualitatively related with those in PFPE's. A systematic study of functional polymeric liquids spreading over solid surfaces with a more elaborate interaction model is currently being investigated.

ACKNOWLEDGMENTS

This research was supported, in part, by the National Science Foundation under Grant No. ECD-8907068. The authors would like to thank Dr. Gary Rauch, Dr. Kevin Grannen, Dr. David Kuo, Dr. Michael Stirniman, and Dr. Samuel Falcone at Seagate Recording Media, and Professor Andrew Gellman at Carnegie Mellon University for useful discussions, and Wei Yang for valuable input to this work. We are also indebted to R. Waltman *et al.* for providing us with a preprint of their paper quoted in Ref. [29].

-
- [1] P. G. de Gennes, *Rev. Mod. Phys.* **57**, 828 (1985).
 - [2] A. M. Cazabat, *Contemp. Phys.* **28**, 347 (1987).
 - [3] P. Ball, *Nature (London)* **338**, 624 (1989).
 - [4] F. Heslot, N. Fraysee, and A. M. Cazabat, *Nature (London)* **338**, 640 (1989).
 - [5] F. Heslot, A. M. Cazabat, and P. Levinson, *Phys. Rev. Lett.* **62**, 1286 (1989).
 - [6] F. Heslot, A. M. Cazabat, P. Levinson, and N. Fraysse, *Phys. Rev. Lett.* **65**, 599 (1990).
 - [7] A. M. Cazabat, N. Fraysee, F. Heslot, and P. Carles, *J. Phys. Chem.* **94**, 7581 (1990).
 - [8] A. M. Cazabat, N. Fraysee, and F. Heslot, *Colloids Surf.* **52**, 1 (1991).
 - [9] M. P. Valignat, N. Fraysee, A. M. Cazabat, and F. Heslot, *Langmuir* **9**, 601 (1993).
 - [10] T. M. O'Connor, M. S. Jhon, C. L. Bauer, B. G. Min, D. Y. Yoon, and T. E. Karis, *Tribol. Lett.* **1**, 219 (1995).
 - [11] T. M. O'Connor, Y. R. Back, M. S. Jhon, B. G. Min, D. Y. Yoon, and T. E. Karis, *J. Appl. Phys.* **79**, 5788 (1996).
 - [12] B. G. Min, J. W. Choi, H. R. Brown, D. Y. Yoon, T. M. O'Connor, and M. S. Jhon, *Tribol. Lett.* **1**, 225 (1995).
 - [13] X. Ma, J. Gui, L. Smoliar, K. Grannen, B. Marchon, C. L. Bauer, and M. S. Jhon, *Phys. Rev. E* **59**, 722 (1999).
 - [14] J. Yang, J. Koplik, and J. R. Banavar, *Phys. Rev. Lett.* **67**, 3539 (1991).
 - [15] J. Yang, J. Koplik, and J. R. Banavar, *Phys. Rev. A* **46**, 7738 (1992).
 - [16] J. A. Nieminen, D. B. Abraham, M. Karttunen, and K. Kaski, *Phys. Rev. Lett.* **69**, 124 (1992).
 - [17] J. A. Nieminen and T. Ala-Nissila, *Phys. Rev. E* **49**, 4228 (1994).
 - [18] J. De Coninck, N. Fraysse, M. P. Valignat, and A. M. Cazabat, *Langmuir* **9**, 1906 (1993).
 - [19] J. De Coninck, S. Hoorelbecke, M. P. Valignat, and A. M. Cazabat, *Phys. Rev. E* **48**, 4549 (1993).
 - [20] J. De Coninck, U. D'Ortona, J. Koplik, and J. R. Banavar, *Phys. Rev. Lett.* **74**, 928 (1995).
 - [21] L. Wagner, *Phys. Rev. E* **51**, 499 (1995).
 - [22] S. Bekink, S. Karaborni, G. Verbist, and K. Esselink, *Phys. Rev. Lett.* **76**, 3766 (1996).
 - [23] A. Lukkarinen, K. Kaski, and D. B. Abraham, *Phys. Rev. E* **51**, 2199 (1995).

- [24] U. D'Ortona, J. De Coninck, J. Koplik, and J. R. Banavar, *Phys. Rev. E* **53**, 562 (1996).
- [25] G. W. Tyndall, T. E. Karis, and M. S. Jhon, Society of Tribologists and Lubrication Engineers Report No. 98-TC-5E-3.
- [26] X. Ma, J. Gui, L. Smoliar, K. Grannen, B. Marchon, M. S. Jhon, and C. L. Bauer, *J. Chem. Phys.* **110**, 3129 (1999).
- [27] P. G. de Gennes, and A. M. Cazabat, *C.R. Acad. Sci., Ser. II: Mech. Phys., Chim. Sci. Terre Univers* **310**, 1601 (1990).
- [28] S. Bardon, M. Cachile, A. M. Cazabat, X. Fanton, M. Valignat, and S. Villette, *Faraday Discuss.* **104**, 1 (1996).
- [29] R. J. Waltman, G. W. Tyndall, and J. Pacansky, *Langmuir* (to be published).
- [30] C. M. Mate and V. J. Novotny, *J. Chem. Phys.* **94**, 8420 (1991).
- [31] C. M. Mate, *Phys. Rev. Lett.* **68**, 3323 (1992).
- [32] R. H. Wang, R. L. White, S. W. Meeks, B. G. Min, A. Kellock, A. Homola, and D. Yoon, *IEEE Trans. Magn.* **32**, 3777 (1996).
- [33] X. Ma, J. Gui, K. Grannen, L. Smoliar, B. Marchon, M. S. Jhon, and C. L. Bauer, *Tribol. Lett.* **6**, 9 (1999).